Available online at www.sciencedirect.com
ScienceDirect
Publishing Services by Elsevier
International Journal of Naval Architecture and Ocean Engineering xx (2017) 1–16
http://www.journals.elsevier.com/international-journal-of-naval-architecture-and-ocean-engineering/

Experimental and numerical study on coupled motion responses of a floating crane vessel and a lifted subsea manifold in deep water

B.W. Nam*, N.W. Kim, S.Y. Hong

Korean Research Institute of Ship & Ocean Engineering, 104 Sinseong-ro, Yuseong-gu, Daejeon 305-343, Republic of Korea

Received 2 September 2016; revised 2 November 2016; accepted 2 January 2017
Available online ■ ■ ■

Abstract

The floating crane vessel in waves gives rise to the motion of the lifted object which is connected to the hoisting wire. The dynamic tension induced by the lifted object also affects the motion responses of the floating crane vessel in return. In this study, coupled motion responses of a floating crane vessel and a lifted subsea manifold during deep-water installation operations were investigated by both experiments and numerical calculations. A series of model tests for the deep-water lifting operation were performed at Ocean Engineering Basin of KRISO. For the model test, the vessel with a crane control system and a typical subsea manifold were examined. To validate the experimental results, a frequency-domain motion analysis method is applied. The coupled motion equations of the crane vessel and the lifted object are solved in the frequency domain with an additional linear stiffness matrix due to the hoisting wire. The hydrodynamic coefficients of the lifted object, which is a significant factor to affect the coupled dynamics, are estimated based on the perforation value of the structure and the CFD results. The discussions were made on three main points. First, the motion characteristics of the lifted object as well as the crane vessel were studied by comparing the calculation results. Second, the dynamic tension of the hoisting wire were evaluated under the various wave conditions. Final discussion was made on the effect of passive heave compensator on the motion and tension responses.

Keywords: Coupled motion; Crane vessel; Subsea manifold; Model test; Lifting operation

1. Introduction

There are various installation methods for subsea equipment in deep water. Conventional crane-wire installation method has been widely used in real-sea operations. For the safety of the crane lifting operations, it is required to check the crane capacity, rigging design and the structural strength of the lifted object. If the weight of the lifted object is considerable, the coupled dynamics of the crane vessel and the lifted object become quite important. Dynamic amplification factor of hook load can be increased by the coupled dynamic effect. As for the subsea installation, the water depth is a critical parameter of the vertical resonance of the hoisting system. Recently, new installation methods such as pendulum installation method, pencil buoy method and sheave method, also have been devised to overcome the limitation or disadvantage of the crane-wire installation method.

A typical crane installation operation in deep water consists of four main phases (DNV, 2011). First phase is lifting off from deck of a transportation barge and maneuvering the object, in which the transient behavior of the lifted object should be suppressed to avoid collision. Second phase is lowering operation through the wave zone. In this stage, various external forces including weight, buoyancy, slamming force, wave force are acting on the lifted object, changing in time according to the lifting locations of the object. The slack condition of the hoisting wires also should be check. Third phase is deep-water lowering (or lifting) operation, in which vertical oscillation of the lifted object can be a significant factor. As the hoisting wire is getting longer, the first eigen

* Corresponding author. Fax: +82 42 866 3919.
E-mail address: bwnam@kriso.re.kr (B.W. Nam).
Peer review under responsibility of Society of Naval Architects of Korea.

http://dx.doi.org/10.1016/j.ijnaoe.2017.01.002

period of the hoisting system can be getting longer up to the operational wave period. In this case, the resonant vertical motions of the lifted object and the large dynamic tension of the hoisting wire can occur during the lowering operation. Final phase is touching down on sea bed and retrieval, which is landing stage. Horizontal offset and motions of the lifted object, which are mainly affected by the low-frequency horizontal motions of the vessel as well as ocean current, can be important considerations related to the accurate positioning of the subsea equipment. Appropriate weather conditions should be screened before the real-sea operation.

During the deepwater lowering or lifting operation, a heave compensation system can be employed to mitigate the vertical resonant motion of the lifted equipment and reduce the dynamic loads in the hoisting wire system. Three types of heave compensators have been used in deep water lifts: Passive, active and combined heave compensators. A Passive Heave Compensator (PHC) is a kind of spring-damper systems which shift resonant frequency of vertical motion of hoisting wire system. The passive heave compensator is also designed to reduce impacts on offshore cranes by adding damping in the hoisting wire. An Active Heave Compensator (AHC) uses either controlled winches or hydraulic pistons, and reference signals. The active heave compensation systems generally use information from vessel Motion Reference Unit (MRU) to control payout length of winch line.

Regarding the real-sea deepwater installation operation of subsea equipment, dynamic analysis method is widely used in design stage to predict the motion responses of the subsea equipment and determine the capacity of the installation equipment and the weather windows. For example, Galgoul et al. (2001) described the analyses and all the problems encountered during the installation project of a PETROBRAS manifold in a 1860 m water depth, at the Roncador field in the Campos Basin, offshore Rio de Janeiro. They also pointed out the axial resonance can be a major concern as the installation depths increase to 3,000 m. Kimiaei et al. (2009) presented a simplified numerical model for the accurate estimation of hydrodynamic forces on subsea platforms and compared the results of the DNV guidelines. They carried out a series of sensitivity analyses using DNV guideline and OrcaFlex models. Vries et al. (2011) described the monitoring campaign on a typical example of a deep water lowering operation. They suggested the monitoring results about the subsea behavior of two suction piles during the installation operation in 2700 m water depth using a support vessel. They also compared the monitoring results with numerical models used for dynamic analysis and concluded that dynamic analysis methods can be applicable to prediction of the motion and load for subsea structure in deepwater installation operation. Legras and Wang (2011) suggested a new method to determine criteria for lowering operations based on real time monitoring of the vessel motion and time-domain simulation. They also described the application of the method on an installation vessel for lowering operations in West Africa. Wang et al. (2011) carried out pipeline installation analysis and jumper lowering analysis by using the commercial software OrcaFlex. They discussed the technical challenges to install the rigid pipeline with PLET, jumper and flying leads. Nam et al. (2013) developed a time-domain analysis program for floating crane vessel systems. They investigated the effect of heave compensator during lowering operation of subsea equipment.

Only a few model tests related to subsea installation or floating crane can be found in literature survey. Clauss et al. (2000) showed an experimental study of the nonlinear dynamics of floating cranes. Fujarra et al. (2008) carried out a seres of simplified model test in order to dimensioning the launching cables and to define the limit environmental conditions for the subsea installation. Nam et al. (2015) performed an experimental study on deepwater crane installation of subsea equipment in waves. They carried out a model test for deepwater lowering and lifting operation of subsea equipment under both regular and irregular wave conditions. They also discussed the effect of passive heave compensator on the deepwater lowering operation of a manifold. To overcome the limitation of water depth in basin, new experimental technique using truncated hoisting system was introduced.

In this study, coupled motion responses of a floating crane vessel and a lifted subsea manifold during deep-water installation operations were investigated. A series of model tests for the deepwater lifting operation were performed at Ocean Engineering Basin of KRISO. To validate the experimental results, a frequency-domain motion analysis was carried out. Under various irregular wave conditions, the motion responses of the vessel as well as the lifted object were examined. The dynamic tension of the hoisting wire were also evaluated under the different wave period conditions. Discussion is made on the effect of passive heave compensator on the motion and tension responses.

2. Model test

2.1. Experimental models

A floating crane vessel named ‘HD2500’, which has been used in real-sea installation project by Hyundai Heavy Industry (HHI), was selected in this model test. The main dimensions of the crane vessel are 130 m(L)*36 m(B) *10.5 m(D). The displacement of the vessel is about 15,000 ton. Fig. 1 shows the image and experimental model for the crane vessel. The scale ratio of the model is 1:50 and the scaled vessel model was made of wood. The crane vessel is equipped with dynamic positioning system for the deepwater operations. Four azimuth thrusters are located at each corner of the vessel. The GM value and roll natural period were adjusted by inclining and free-decay tests. The pitch gyration was measured with a swing table test. There is a single crane system with maximum capacity 2500 ton on the deck of the vessel.

Among various types of subsea equipment, a typical subsea manifold was considered in this model test. Fig. 2 shows CAD image and experimental model of the manifold. The present manifold has complex geometry, which consists of complex

Please cite this article in press as: Nam, B.W., et al., Experimental and numerical study on coupled motion responses of a floating crane vessel and a lifted subsea manifold in deep water, International Journal of Naval Architecture and Ocean Engineering (2017), http://dx.doi.org/10.1016/j.ijnaoe.2017.01.002

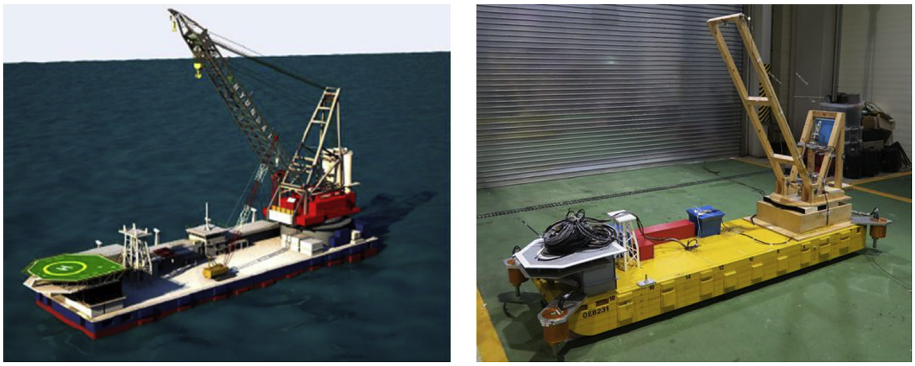

Fig. 1. Image (left) and experimental model (right) for the floating crane vessel.

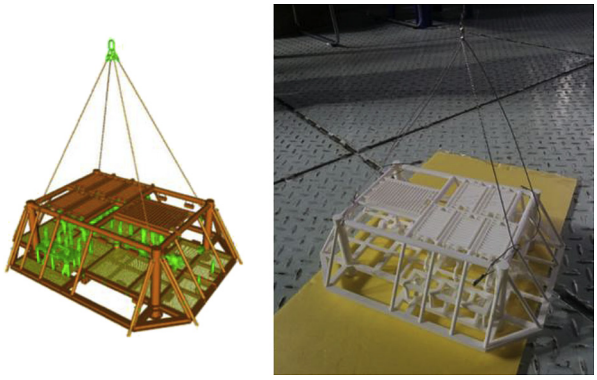

Fig. 2. Experimental models for the subsea manifold.

porous plates and truss frames. The main dimension of the manifold is 15.6 m(L)*12.3 m(B)*4.3 m(D). The air weight of the manifold is about 150 ton. The experimental model of the manifold was made of plastic material by using 3-D printing techniques. In order to adjust the model weight, the additional lead weights are put inside the model of the manifold. Table 1 summarized the main dimensions of the crane vessel and the manifold.

Table 1
Main dimensions of the installation vessel and the subsea equipment.

Item	Installation vessel	Manifold
L	130.0 m	15.6 m
B	36.0 m	12.3 m
D	10.5 m	4.3 m
Weight	Abt 15,000 ton	Abt. 150 ton

2.2. Crane system and passive heave compensator

The crane system is consisted of three main parts, i.e. boom, backstay and crane base. Fig. 3 shows CAD image and experimental model of the crane system in which the main crane frame is made of wood. The electric motors are utilized for hoisting wire and boom rotation. The crane control motor is connected to winch drum via reduction gear and coupling, shown in Fig. 4. In this study, the hoisting wire tension was measured by using 1-axis loadcell and pulley system. To match the vertical natural period of the hoisting system, the axial stiffness of the hoisting wire in the model scale should be equivalent to that of the real system. In this study, several nylon lines for fishing were tested and then the most appropriate one was chosen.

Passive heave compensator can be modeled as additional spring and damper. Fig. 5 shows a photo and schematic diagram of the passive heave compensator. It is well-known that the passive heave compensator reduces peak heave and tension response of the hoisting system by shifting the resonant period (Nam et al., 2013). Although actual passive heave compensator has nonlinear spring and damping characteristics, a linear

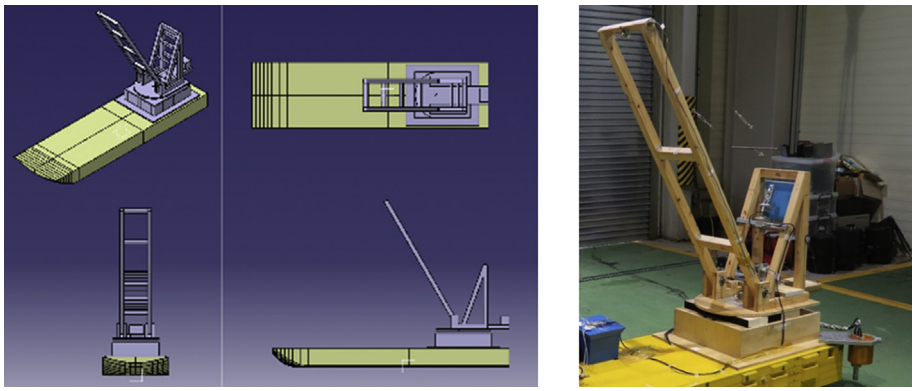

Fig. 3. CAD model (left) and experimental model of the crane system.

Please cite this article in press as: Nam, B.W., et al., Experimental and numerical study on coupled motion responses of a floating crane vessel and a lifted subsea manifold in deep water, International Journal of Naval Architecture and Ocean Engineering (2017), http://dx.doi.org/10.1016/j.ijnaoe.2017.01.002

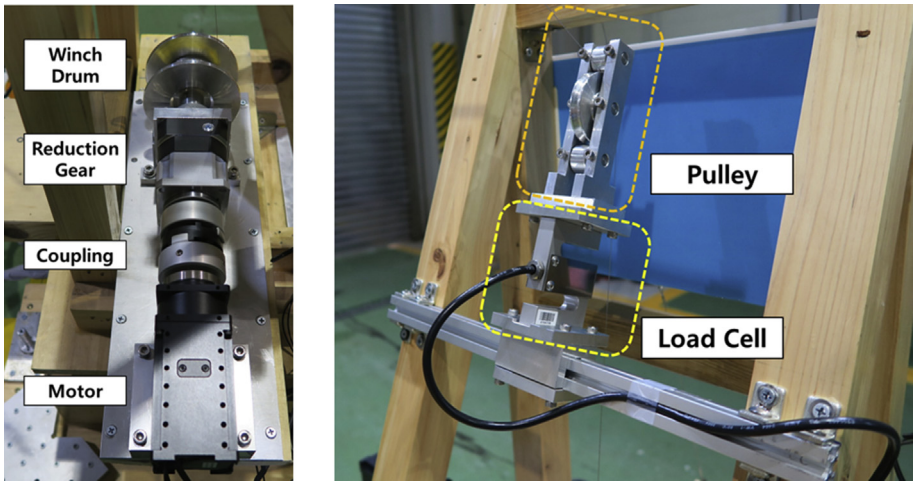

Fig. 4. Crane control motor (left) and tension measurement system (right).

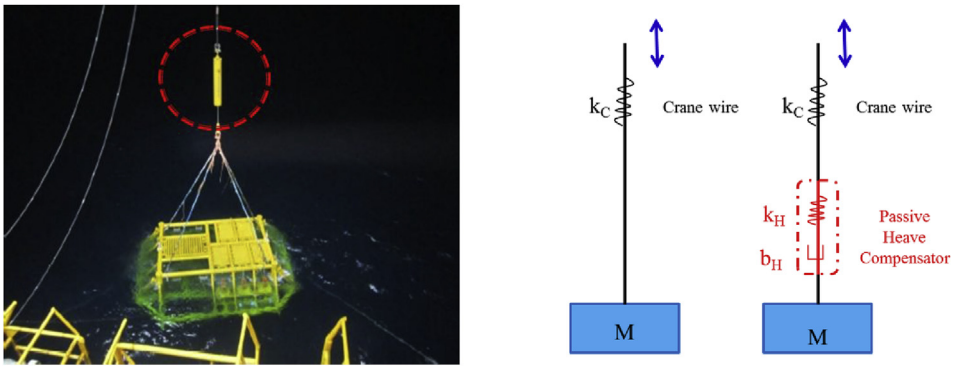

Fig. 5. Photo (left) and schematic diagram (right) of passive heave compensator.

spring can be used to investigate the fundamental effect of passive heave compensator. In this study, passive heave compensator is modeled as a linear spring, while damper is not considered.

2.3. Experimental conditions and measurement

First, a white noise test was carried out to evaluate the motion and tension RAOs. Then the coupled motion responses of the vessel and the lifted manifold were examined under various irregular wave conditions. Fig. 6 shows white noise and irregular wave spectra which have been used in the present model test. Irregular wave conditions are summarized in Table 2. The wave spectra used in this study are ITTC spectra. The significant wave height is fixed as 1.0 m because the installation operation is normally performed under the mild ocean environment when the significant wave height is less than 1.0 m or 1.5 m. The wave periods range from 4.0 s to 14.0 s.

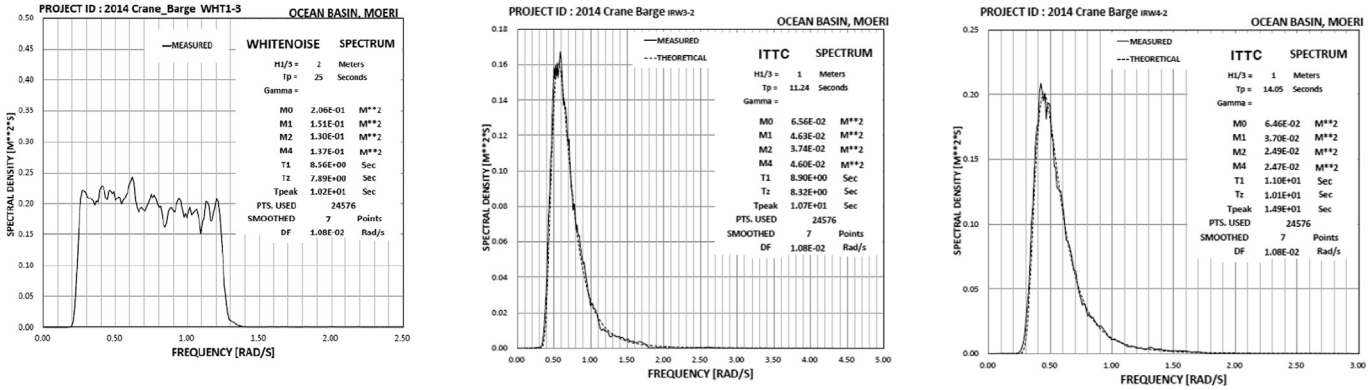

(a) White noise spectrum (b) IRW03 (c) IRW04

Fig. 6. White noise and irregular wave spectra.

Please cite this article in press as: Nam, B.W., et al., Experimental and numerical study on coupled motion responses of a floating crane vessel and a lifted subsea manifold in deep water, International Journal of Naval Architecture and Ocean Engineering (2017), http://dx.doi.org/10.1016/j.ijnaoe.2017.01.002

Table 2
Irregular wave conditions.

Wave ID	Spectrum	Tz (sec)	Tp (sec)	Hs (m)
IRW01	ITTC	4.000	5.620	1.000
IRW02	ITTC	6.000	8.429	1.000
IRW03	ITTC	8.000	11.239	1.000
IRW04	ITTC	10.000	14.049	1.000
IRW05	ITTC	12.000	16.859	1.000
IRW06	ITTC	14.000	19.669	1.000

The wave periods longer than 10 s are less meaningful for normal installation sites. However, for some specific installation areas, the swell conditions of long wave periods can be critical for the installation operations. In addition, we want to evaluate PHC performance under wide-range period conditions.

In order to measure the motion of the lifted subsea equipment in water, a underwater jig and two cameras were introduced in this model test, shown in Fig. 7. The underwater jig was installed in the pit at water depth of −700 m. A black ball maker is attached to the subsea equipment in order to capture the motion of the lifted object by applying image processing. Fig. 8 shows the typical motion trajectories of the lifted manifold extracted from the recorded experimental movie.

3. Numerical analysis

3.1. Equation of motion

In this study, it is assumed that the crane vessel experience 6-dof motions and the lifted object is subjected to only 3-dof translation motions. Total coupled motion equations can be expressed like followings;

$$\left\{-\omega^2\begin{bmatrix}\mathbf{M}_V+\mathbf{A}_V(\omega) & 0_{6\times3}\\ 0_{3\times6} & \mathbf{M}_S+\mathbf{A}_S\end{bmatrix}-i\omega\begin{bmatrix}\mathbf{B}_V^{pot}(\omega) & 0_{6\times3}\\ 0_{3\times6} & \mathbf{B}_S^{vis}\end{bmatrix}\right\}\times\begin{Bmatrix}\xi_V\\ \xi_S\end{Bmatrix}+\begin{bmatrix}\mathbf{C}_V^{hydro}+\mathbf{C}_V^{wire} & \mathbf{C}_{VS}^{wire}\\ \mathbf{C}_{SV}^{wire} & \mathbf{C}_S^{wire}\end{bmatrix}\begin{Bmatrix}\xi_V\\ \xi_S\end{Bmatrix}=\begin{Bmatrix}\mathbf{F}_V(\omega)\\ 0_{3\times3}\end{Bmatrix} \quad (1)$$

Where, $\mathbf{M}_V$ and $\mathbf{M}_S$ are the inertia matrix of the vessel and the lifted structure, respectively. $\mathbf{A}_V(\omega)$ and $\mathbf{B}_V^{pot}(\omega)$ are the added-mass matrix and potential damping matrix of the vessel, which are basically functions of the motion frequency. These added-mass and potential damping coefficients of the surface vessel can be easily evaluated by applying conventional wave Green function method with boundary element method. In this study, higher-order boundary element method is applied to obtain the added-mass and damping coefficients of the vessel. $\mathbf{A}_S$ and $\mathbf{B}_S^{vis}$ are the added-mass matrix and the viscous damping matrix of the lifted structure. If the lifting location is deep enough, the added-mass of the lifted structure can be assumed to be constant and potential damping is negligible. In this case, additional damping due to the viscous drag force becomes significant compared to the potential damping. In this study, linearized viscous damping is considered. $\mathbf{C}_V^{hydro}$ is the hydrodynamic restoring matrix. $\mathbf{C}_V^{wire}$, $\mathbf{C}_S^{wire}$, $\mathbf{C}_{VS}^{wire}$, $\mathbf{C}_{SV}^{wire}$ are the linear spring matrix due to the crane wire, which connects the vessel and the lifted structure.

3.2. Hydrodynamic coefficient of the manifold

The motion response of the lifted object in water are quite dependent on the hydrodynamic forces which can be decomposed into added-mass and hydrodynamic damping forces.

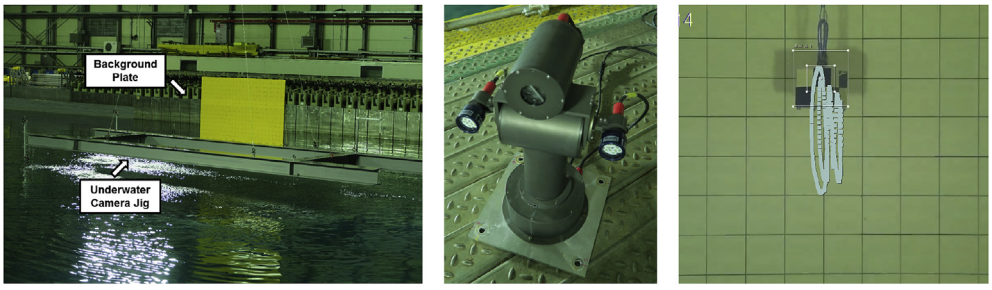

Fig. 7. Underwater jig (left), camera (middle) and image processing results (right).

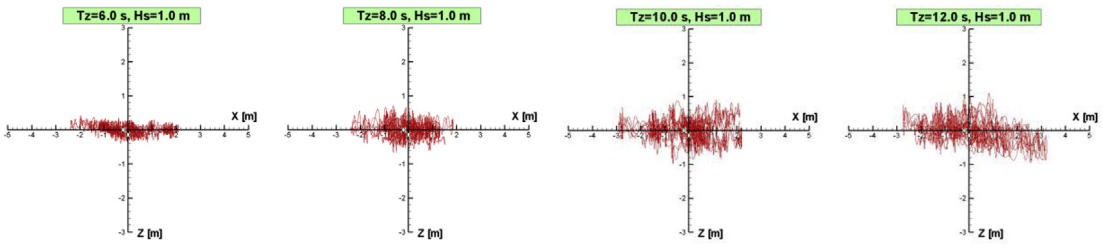

Fig. 8. Motion trajectories of the lifted subsea manifold under the irregular wave conditions (water depth = −700 m).

Please cite this article in press as: Nam, B.W., et al., Experimental and numerical study on coupled motion responses of a floating crane vessel and a lifted subsea manifold in deep water, International Journal of Naval Architecture and Ocean Engineering (2017), http://dx.doi.org/10.1016/j.ijnaoe.2017.01.002

The added-mass values of the submerged object is mainly determined of the object shape. Since the manifold has complex truss frame and porous plate, it can be predicted that the weight in water of the manifold can increases significantly rather than the weight in air. However, it is hard to estimate the added-mass values of this kind of complex geometry. In this study, in order to estimate the added-mass of the manifold, the extrapolation method based on the structure perforation is applied. Fig. 9 shows the several manifold geometry with different perforation values. Fig. 10 shows the added-mass ratios according to the structure perforation values with respect to the solid structure with no perforation. The computational results are compared with the simplified estimation formula which was suggested by DNV (2011). Based on these calculation results, the estimated added-mass ratio ranges around 10%–20% of the added-mass at the solid manifold given in Fig. 9(a). In the later calculations, the added-mass of the manifold is assumed as about 128 ton, which corresponds to 15% of the added-mass of the solid manifold with no perforation.

To estimate the drag coefficient of the subsea manifold, CFD calculations were carried out by using commercial CFD software (Park et al., 2013). Fig. 11 shows the CFD simulation results in two opposite inflow angles. Based on the CFD results, the drag coefficient (C_D) is about 0.722, where the projection area(A_P) is 192.0 m^2. In this case, quadratic heave damping coefficient (b_{99}^{non}) is about 70 $kN \cdot s^2/m^2$. The equivalent linear heave damping coefficients (b_{99}^{eq}) are shown in Fig. 12. In principle, the equivalent linear damping coefficient varies with excitation frequency and motion amplitude. As shown in figure, the equivalent damping coefficient ranges from 50 $kN \cdot s/m$ to 250 $kN \cdot s/m$.

4. Results & discussions

In this study, a series of model tests were performed to evaluate deep-water crane operation of lifting the subsea manifold. Fig. 13 shows photos for the floating crane vessel and the lifted subsea equipment during the model test. The pit in the center of the basin was utilized to ensure the enough water depth. The crane vessel was positioned so that the lowering position was located in the center of the pit. Considering the scale ratio, the maximum water depth of the basin was equivalent to 700 m in real scale. The dynamic positioning system was used for the crane vessel without mooring system, where proportional gains of the DP system

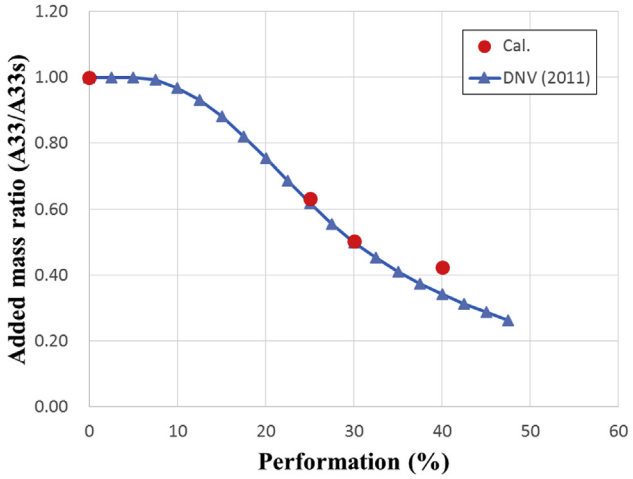

Fig. 10. Added mass ratio values according to structure perforation.

were set as the natural periods of horizontal vessel motions became around 200 s. In this study, only port-side lifting operations with single hoisting wire were taken into account. Black ball makers, shown in Fig. 13(b), were attached to the manifold for the motion capturing by using image processing.

4.1. Motion responses of the installation vessel

The motion RAOs of the crane vessel, shown in Fig. 14, were obtained from the white noise test during the lifting operation of the subsea manifold. In this case, the lifting location is about −700 m under the still water and wave heading is 180°. For the comparison, the frequency-domain calculation results are also plotted together with the experimental data. Heave and pitch RAOs show typical motion responses of the barge vessel under the head sea conditions. The maximum pitch motion of the vessel is about 1.3° per unit incident amplitude when the wave frequency is around 0.6 rad/s. If the wave length is similar to the vessel length at around 0.8 rad/s, the pitch motion slightly decreases due to the cancelation effect and the heave motion locally increases. The secondary pitch peak can be also found 0.9 rad/s. What is noticeable in the vessel motion is that the significant roll motions occur even in the head waves. This is because the interaction with the lifted object via the hoisting wire tension brings about the roll motions of the crane vessel. The roll resonance of the crane vessel happens at around 0.60 rad/s and the maximum roll motion is about 0.8° per unit incident

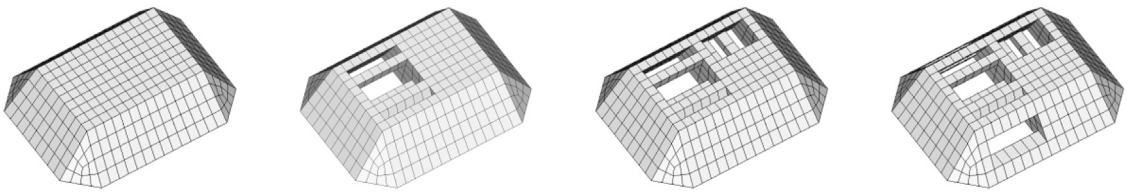

(a) 0% (b) 25% (c) 30% (d) 40%

Fig. 9. Various manifold geometry with different perforation.

Please cite this article in press as: Nam, B.W., et al., Experimental and numerical study on coupled motion responses of a floating crane vessel and a lifted subsea manifold in deep water, International Journal of Naval Architecture and Ocean Engineering (2017), http://dx.doi.org/10.1016/j.ijnaoe.2017.01.002

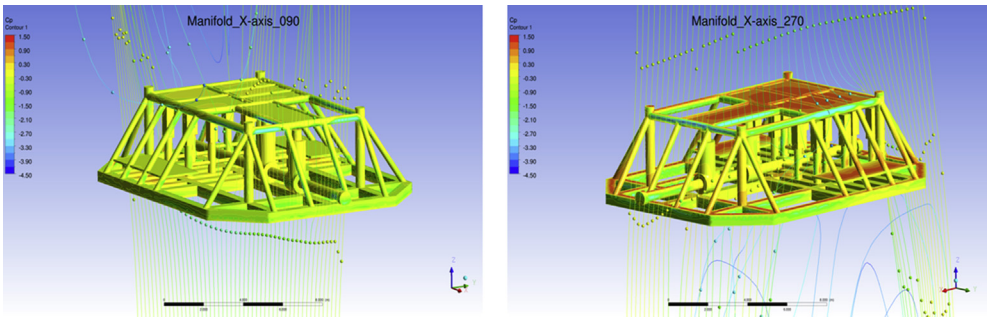

Fig. 11. CFD simulation results of the streamlines and pressure contour around the manifold in uniform flow.

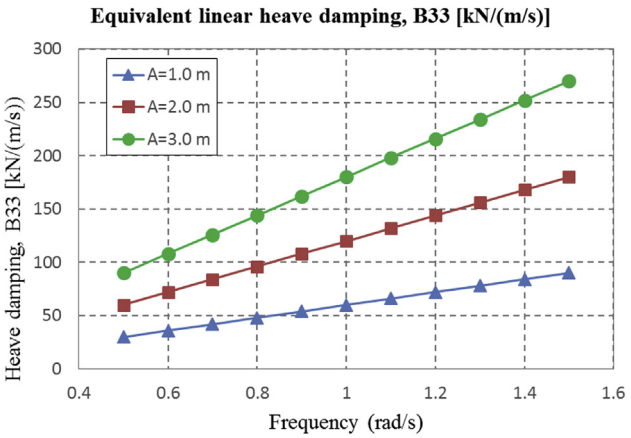

Fig. 12. Added mass values according to structure porosity.

amplitude. In the roll motion RAOs, considerable discrepancies can be found between experiments and calculations at the wave frequency lower than 0.5 rad/s. At around 0.3 rad/s, the roll RAO values become less accurate because of the reduced wave energy. In addition, it can be understood that the more roll motions are induced because the experimental models cannot be perfectly arranged along the incoming waves.

It is noteworthy that the roll motion can be strongly affected by the weight of the lifted object. Fig. 15 shows the effect of the manifold weight on the roll responses of the crane vessel. As the manifold is getting heavier, the roll motion of the crane vessel also increases especially near the roll and pitch natural period.

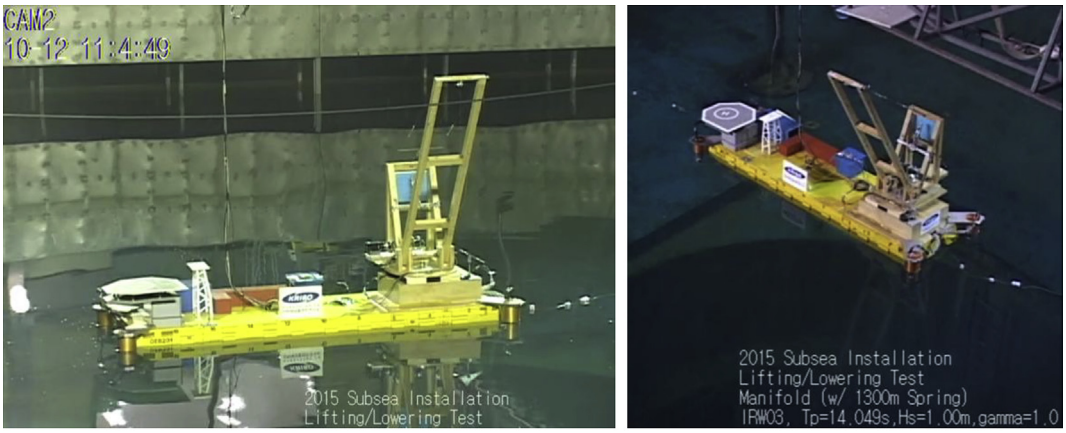

(a) Floating crane vessel

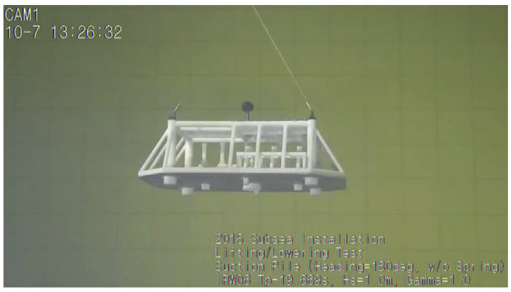

(b) Subsea manifold

Fig. 13. Photos for deep-water lifting experiments with a floating crane vessel and a subsea manifold.

Please cite this article in press as: Nam, B.W., et al., Experimental and numerical study on coupled motion responses of a floating crane vessel and a lifted subsea manifold in deep water, International Journal of Naval Architecture and Ocean Engineering (2017), http://dx.doi.org/10.1016/j.ijnaoe.2017.01.002

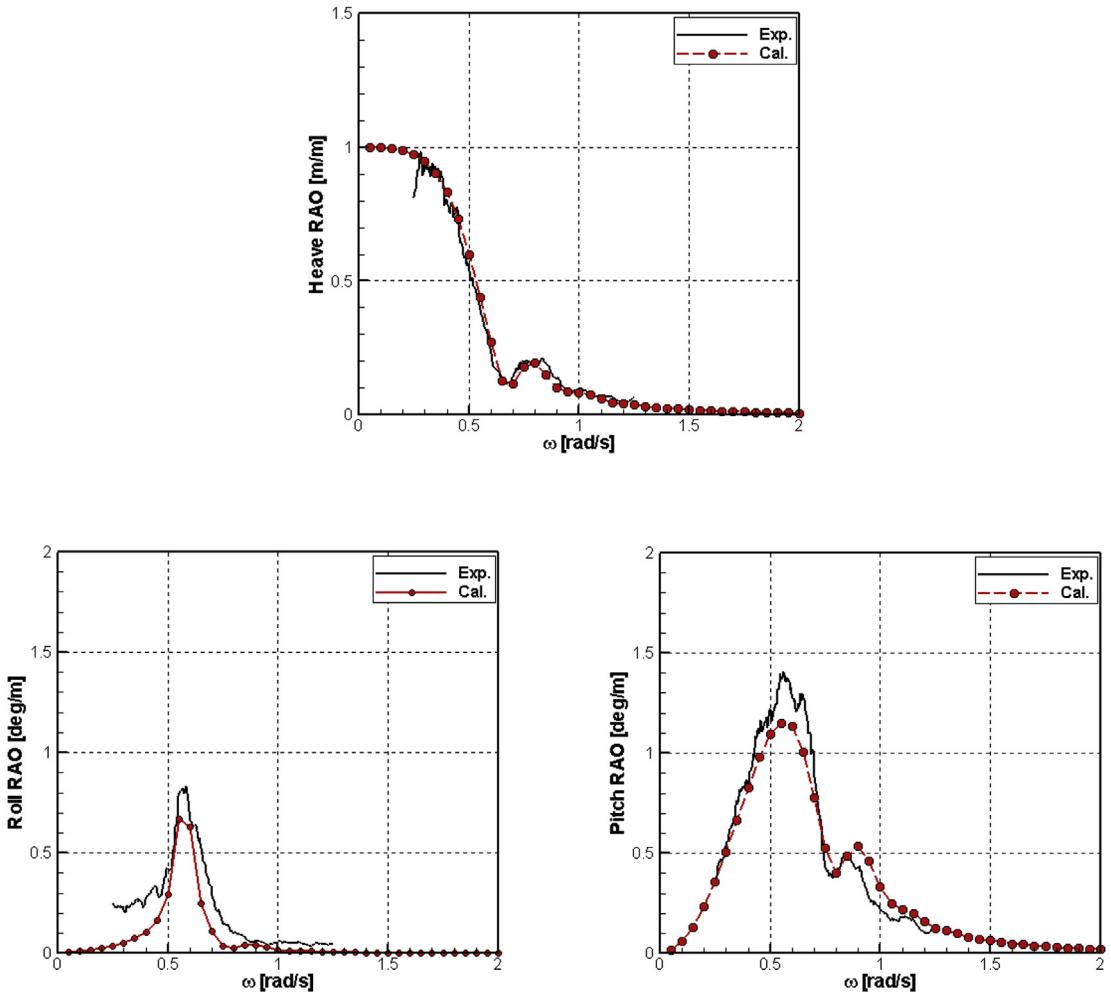

Fig. 14. Motion RAOs of the crane vessel during the lifting operation of the subsea manifold.

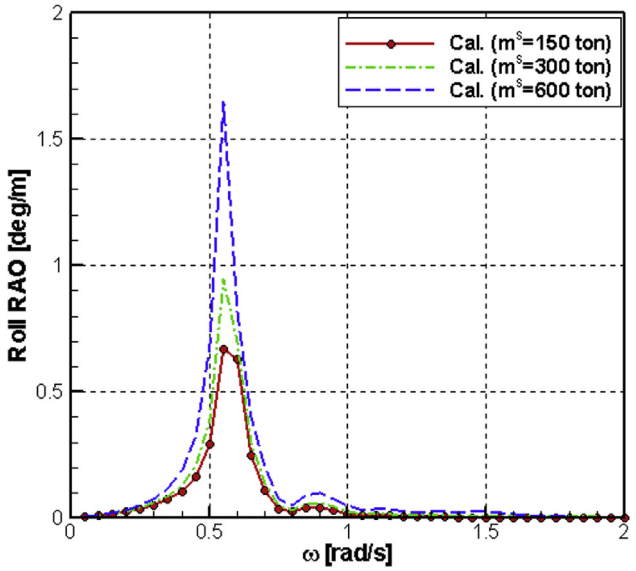

Fig. 15. Effect of the manifold weight on roll RAOs of the crane vessel.

Fig. 16 compares the motion Root Mean Square (RMS) values of the crane vessel under five different irregular wave conditions. The heave responses of the vessel increases as the wave period is getting longer. Roll and pitch motions maximized when the wave period is 10.0 s that is close to the natural period of roll and pitch motions. For all cases, the heave response is less than 0.25 m and angular motions are less than 0.3°. Calculation results show good agreements with the experimental data in heave and pitch responses of the vessel. However, it can be observed that there are some discrepancy in roll motions especially near the roll natural period. These discrepancies are partly attributed to the roll viscous damping of the vessel and the nonlinear heave damping of the lifted object.

4.2. Motion responses of the lifted object

The heave motion RAO of the lifted subsea manifold from the model test is shown in Fig. 17 with the comparison of the calculation results. It can be observed that there are three different peaks in heave responses of the lifted manifold. First

Please cite this article in press as: Nam, B.W., et al., Experimental and numerical study on coupled motion responses of a floating crane vessel and a lifted subsea manifold in deep water, International Journal of Naval Architecture and Ocean Engineering (2017), http://dx.doi.org/10.1016/j.ijnaoe.2017.01.002

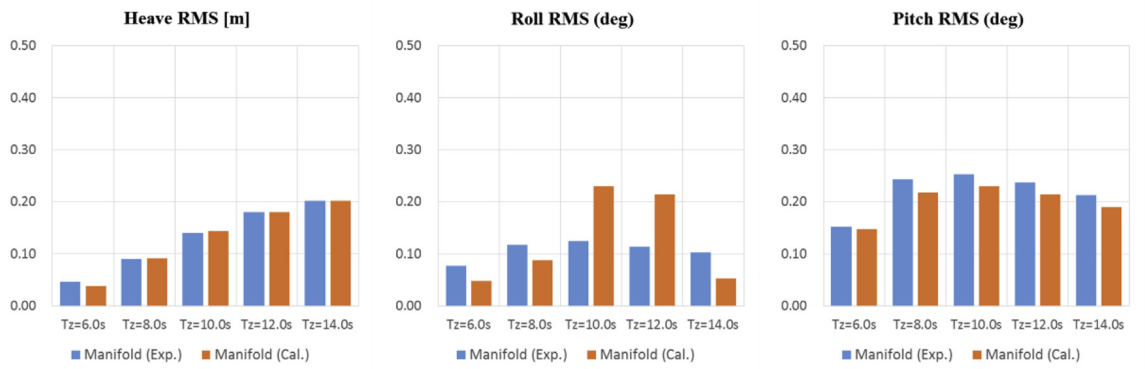

Fig. 16. Motion RMS values of the installation vessel during lifting the subsea equipment.

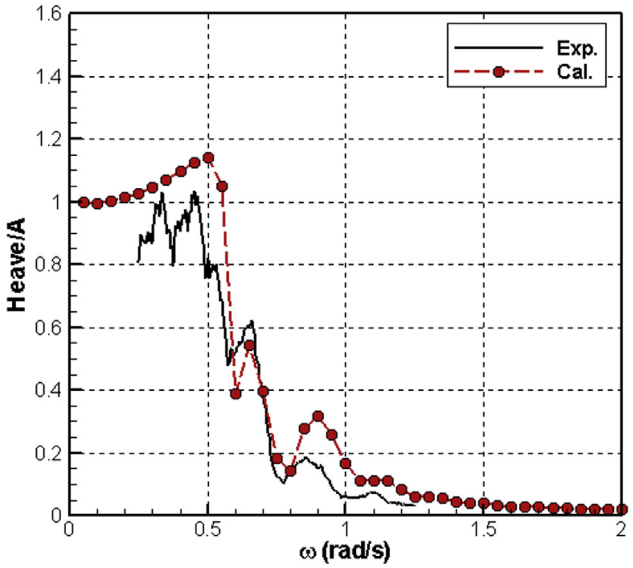

Fig. 17. Heave motion RAO of the lifted subsea manifold during the deep-water lifting operation.

peak can be found at around 0.5 rad/s where the coupled heave and pitch motions of the crane vessel cause a large vertical motion of the crane tip. There are second peak at around 0.6 rad/s which is close to pitch and roll natural frequencies. The last peak is located at around 0.9 rad/s. This peak is induced by the vertical resonance of the hoisting system. Overall comparison between experiments and calculations shows fairly good agreement. However, there are some discrepancies especially in high frequency regions, in which the constant equivalent linear damping coefficient results in relatively less damping force rather than quadratic drag force. To estimate the motion responses of the lifted object, the appropriate estimation of the hydrodynamic coefficient is critical. It can be expected that the motion responses of the lifted object are strongly affected by the added-mass and hydrodynamic damping of the lifted object. Fig. 18(a) shows the damping effect on the motion responses of the lifted object. As the hydrodynamic damping increases, the motion responses of the lifted object decreases. In particular, the motion responses around 0.5 rad/s are greatly reduced due to the increase of the damping. Fig. 18(b) shows the added-mass effect on the motion responses of the lifted object. In this case, the added-mass values are changed according to the perforation percentage. It can be seen that as the added-mass increases, the motion responses of the lifted object also largely increased.

Left figures in Fig. 19 shows the original heave time series of the lifted manifold in irregular waves. What is clearly observed from these figures is that the lifted object experiences both wave-frequency and low-frequency heave motions. The wave-frequency heave motion of the lifted object is directly generated by the hoisting system dynamics excited by the crane tip heave motion. In addition, it can be understood that large surge motion causes the low-frequency heave motion of the lifted object because the manifold is lifted with a long crane wire similar to the pendulum. The right figures in Fig. 17 are the wave-frequency component of heave motions by applying a band-pass filter. As the wave period increases, the heave motions also slightly increase. When the zero-upcrossing wave period is 8.0 s, the maximum heave amplitude of the wave-frequency component is about 0.5 m. If the wave period becomes 14.0 s, the maximum heave amplitude of the wave-frequency component is about 0.7 m.

The direct comparisons of the heave response spectra of the lifted manifold between experimental data and calculation results are shown in Fig. 20. It can be clearly observed that as the wave period is getting longer, the spectrum area increases. All the motion spectra also reveals not only the wave-frequency component but also low-frequency component. As for the wave-frequency component, the calculations predict similar motion response spectra for all wave periods. However, the calculation results gives slight bigger motion spectra rather than experiments. It can be understood that nonlinear hydrodynamic damping characteristics gives discrepancy between the calculations and the experiments. Fig. 21 compares the RMS values of the heave motions of the lifted manifold. Overall trends are quite similar between experiments and calculations. As the damping force increase, it can be found that the numerical estimations is getting closer to the experimental data.

Please cite this article in press as: Nam, B.W., et al., Experimental and numerical study on coupled motion responses of a floating crane vessel and a lifted subsea manifold in deep water, International Journal of Naval Architecture and Ocean Engineering (2017), http://dx.doi.org/10.1016/j.ijnaoe.2017.01.002

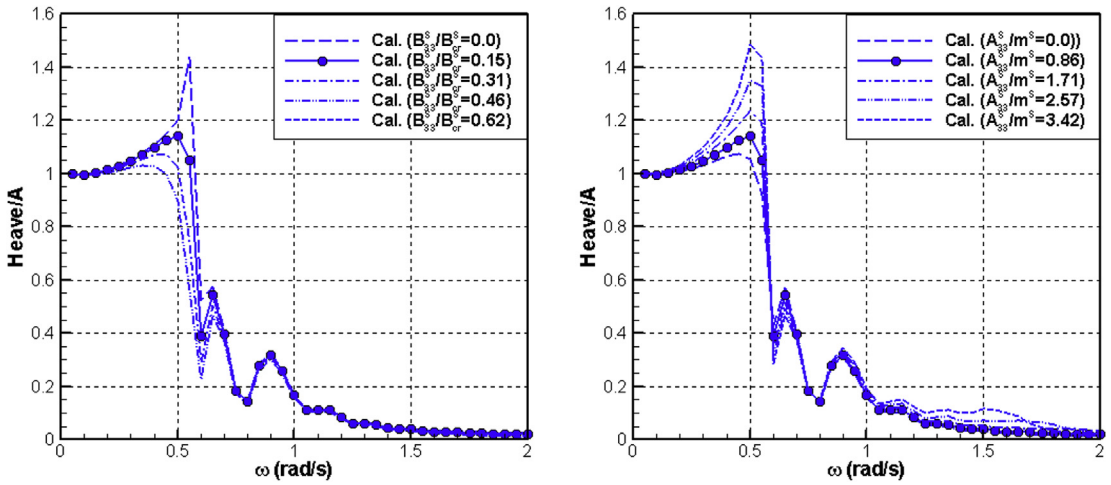

(a) Damping Effect (b) Added-mass effect (Perforation)

Fig. 18. Heave responses spectra of the crane tip and lifted subsea equipment during the deep-water lifting operation in irregular waves.

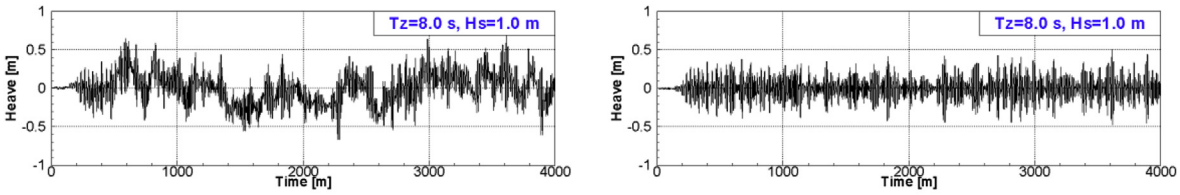

(a) Tz=8.0 s, Hs=1.0 m

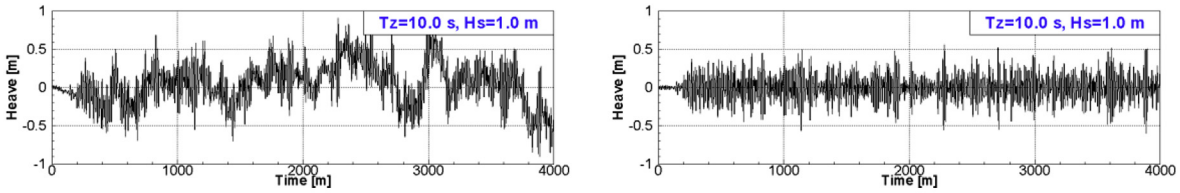

(b) Tz=10.0 s, Hs=1.0 m

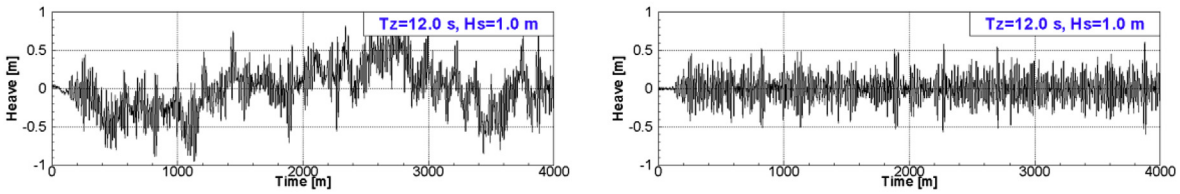

(c) Tz=12.0 s, Hs=1.0 m

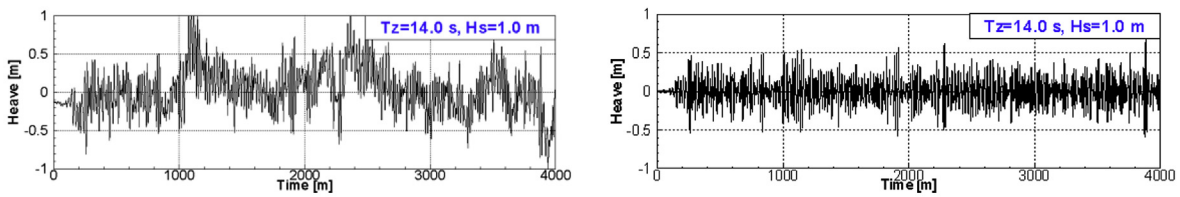

(d) Tz=14.0 s, Hs=1.0 m

Fig. 19. Heave time series of the manifold during the deep-water lifting operation in irregular waves (Manifold, water depth = −700 m).

Please cite this article in press as: Nam, B.W., et al., Experimental and numerical study on coupled motion responses of a floating crane vessel and a lifted subsea manifold in deep water, International Journal of Naval Architecture and Ocean Engineering (2017), http://dx.doi.org/10.1016/j.ijnaoe.2017.01.002

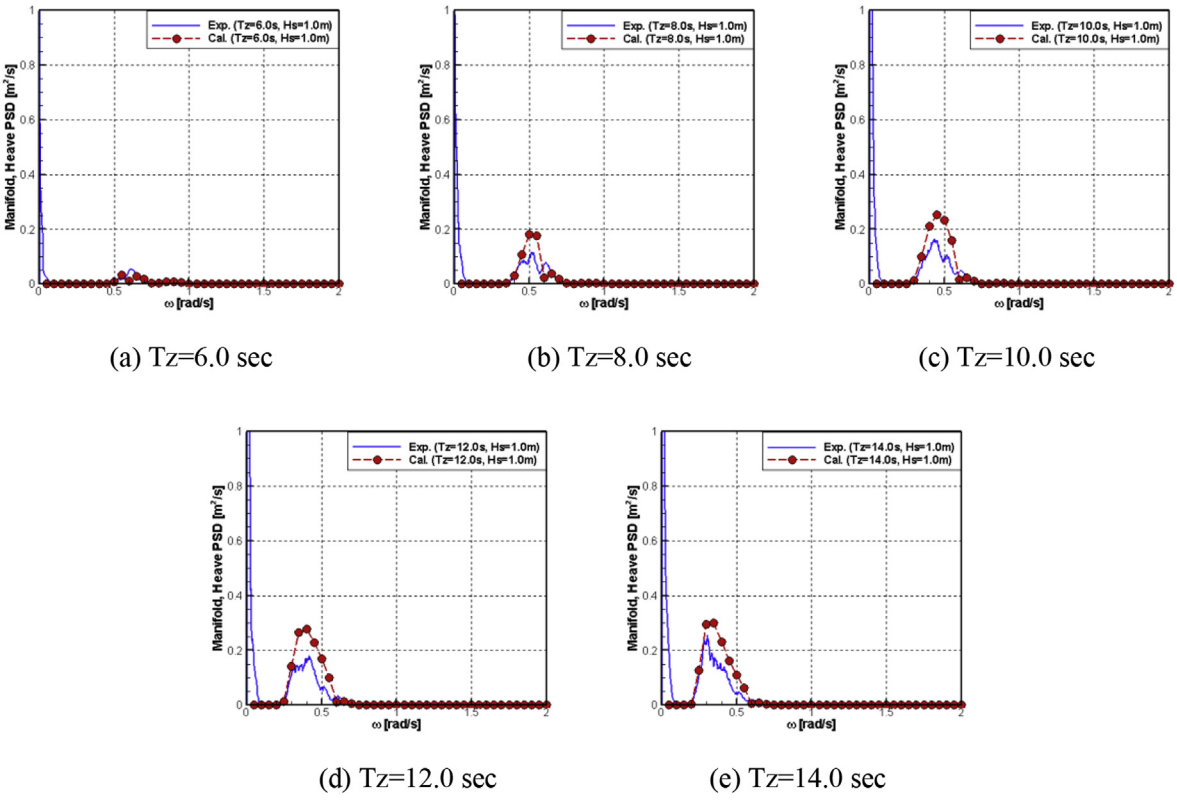

(a) Tz=6.0 sec (b) Tz=8.0 sec (c) Tz=10.0 sec

(d) Tz=12.0 sec (e) Tz=14.0 sec

Fig. 20. Comparison of heave responses spectra of the lifted manifold in irregular waves.

Fig. 22 shows estimated heave motion responses of the lifted subsea manifold under various wave height conditions. As the wave period is getting longer, the heave motion responses of the lifted manifold increase. If the wave period is enough long, heave SDA (Significant Double Amplitude) value is similar to the significant wave height of the incident wave spectrum. This means that the motion response of the lifted object is similar to the incident wave elevations as the wave period is getting longer.

4.3. Dynamic tension of hoisting wire

The dynamic tension of the hoisting wire is determined by relative heave motion between the crane tip and the lifted object. Thus, the dynamic tension RAOs of the hoisting wire are largely affected by the motion response of the lifted object. Fig. 23 compares the tension RAOs between the experiments from the white noise test and calculation results. Similar to the heave motion RAOs of the lifted manifold, the tension RAOs also shows three peak responses. The maximum dynamic tension is about 18 tonf which is correspond to 12% of the

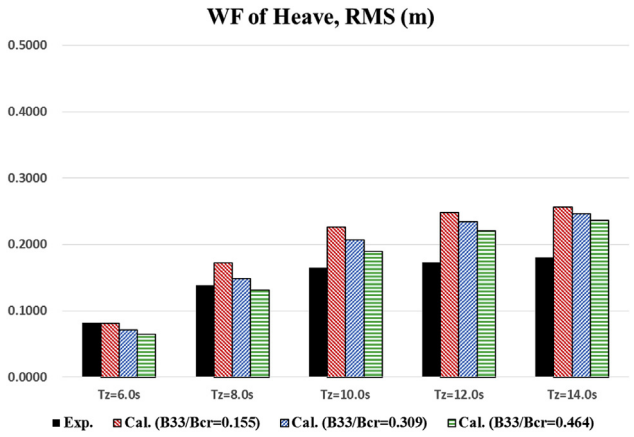

Fig. 21. Comparison of the wave-frequency heave RMS values of the lifted subsea equipment under the irregular wave conditions.

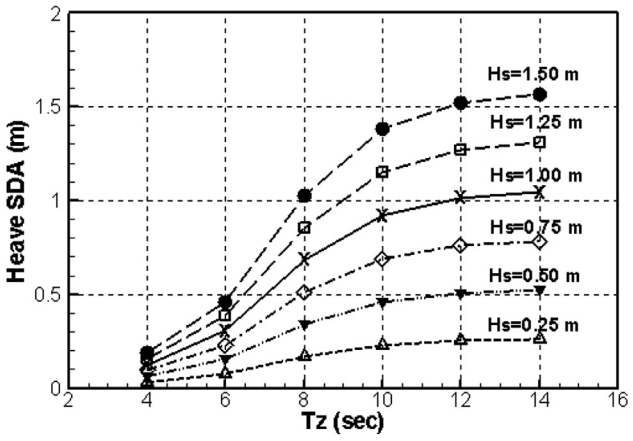

Fig. 22. Estimated heave motion responses of the lifted subsea manifold under various wave height conditions.

Please cite this article in press as: Nam, B.W., et al., Experimental and numerical study on coupled motion responses of a floating crane vessel and a lifted subsea manifold in deep water, International Journal of Naval Architecture and Ocean Engineering (2017), http://dx.doi.org/10.1016/j.ijnaoe.2017.01.002

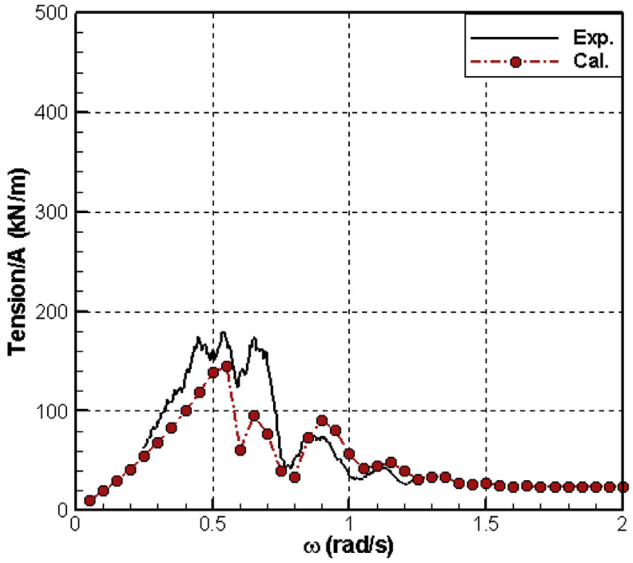

Fig. 23. Tension RAOs of the hoisting wire during the lifting operations.

manifold weight in air. Maximum dynamic tension happens at around 0.6 rad/s which is close to the pitch and roll resonant conditions. As shown in the figure, another peak response can be found at around 0.9 rad/s. These second peak is attributed to the vertical resonance of the hoisting system which is dependent on the hoisting wire stiffness and the lifted object weight. The dynamic tension response of the hoisting wire also can be changed by the hydrodynamic coefficient of the lifted object. Fig. 24 shows the effect of added-mass and hydrodynamic damping on the tension RAOs of the hoisting wire during the lifting operation.

Figs. 25 and 26 show the time series and spectra of the dynamic tension of the hoisting wires under the irregular wave conditions, respectively. As the wave period is getting longer, the tension response spectrum is also shifted to the low frequency ranges. When the wave period is 10.0 s, the tension response is maximized. The overall calculations results of the tension spectra are quite similar trends to the experimental data. In Fig. 27, the significant positive amplitudes of the hoisting wire tension are compared between experiments and calculation results. In this study, zero-upcrossing analysis method is applied to extract the statistical values from the tension time series. The comparison shows quite good agreement.

4.4. Effect of passive heave compensator

The performance of the passive heave compensator (PHC) is quite dependent on the spring and damping characteristics of the PHC system. Left figures of Fig. 28 show the heave RAOs of the manifold from the model tests when the three different passive heave compensators are applied. In this case, 'PHC1', 'PHC2' and 'PHC3' have the stiffnesses of 120 kN/m, 250 kN/m and 490 kN/m, respectively. 'PHC1' has relatively softer stiffness rather than 'PHC2' and 'PHC3'. When 'PHC1' is used, it can be clearly seen that the passive heave compensator is effectively working, in which the usage of the passive heave compensator reduces the heave motion if the wave frequency is higher than 0.4 rad/s. However, when 'PHC2' or 'PHC3' is used, the effect of the passive heave compensator is not clearly seen and the heave motions of the lifted manifold increase instead. Similar to the experimental data, calculation results also indicate that the usage of 'PHC1' only reduces the heave motion of the lifted manifold.

The effect of passive heave compensator can also be found in tension RAOs shown in Fig. 29. While 'PHC2' and 'PHC3' increases the tension response of the crane wire, only 'PHC1' greatly reduces the tension responses for all frequency ranges. The calculation results also demonstrates that only 'PHC1' is effective to reduce the dynamic tension of the crane wire. There results indicate the optimal design of the passive heave compensator is critical factor when we consider the passive heave compensator in the crane lifting operation.

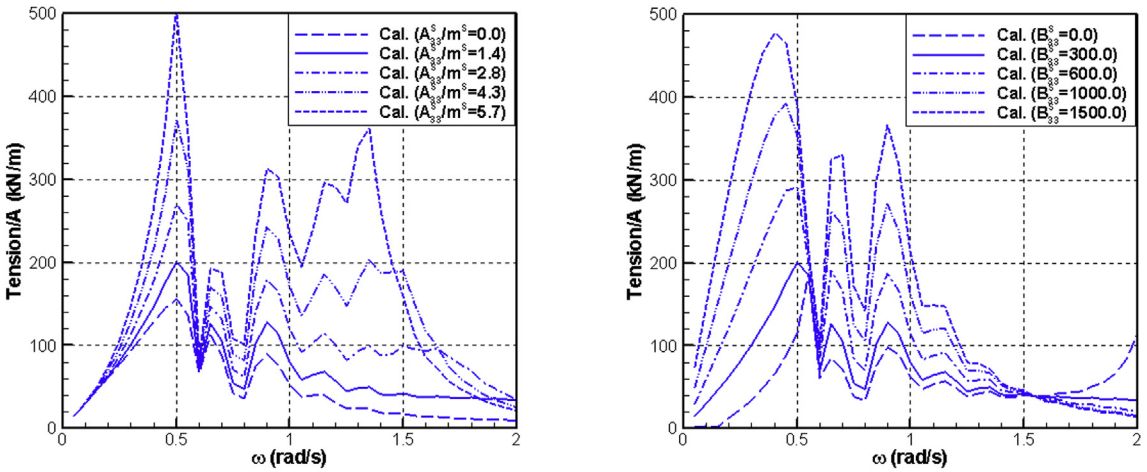

(a) Added-mass Effect (b) Damping effect

Fig. 24. Tension RAOs of the hoisting wire during the lifting operations.

Please cite this article in press as: Nam, B.W., et al., Experimental and numerical study on coupled motion responses of a floating crane vessel and a lifted subsea manifold in deep water, International Journal of Naval Architecture and Ocean Engineering (2017), http://dx.doi.org/10.1016/j.ijnaoe.2017.01.002

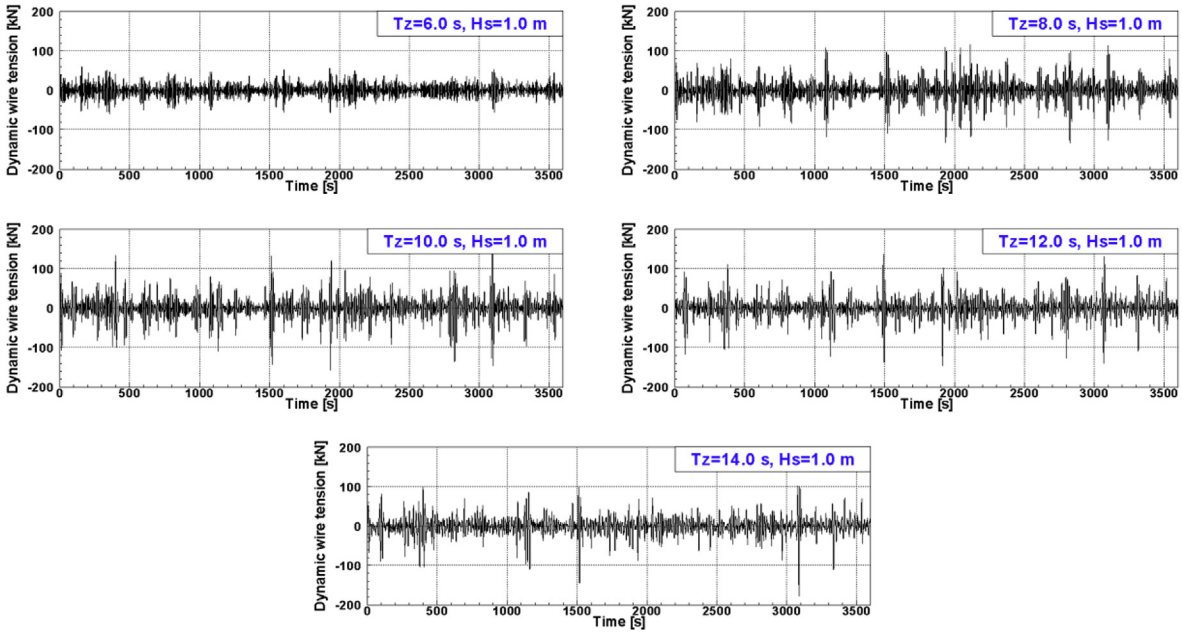

Fig. 25. Time series of the dynamic tension of the hoisting wires during the lifting operation under the irregular wave conditions (water depth = −700 m).

Fig. 30 shows the effect of the passive heave compensator by showing the direct comparison of the heave time series of the manifold and the dynamic tensions of the hoisting wires under three different irregular wave conditions. Relatively, heave compensation effect is not clearly observed for all wave conditions. Whereas, the dynamic tension of the hoisting wires are significantly reduced if the wave period is less than 10.0 s.

Fig. 31(a) compares the heave RMS values of the manifold and dynamic tension responses of the hoisting wire under five different irregular wave conditions from the model tests. As can be seen, the heave compensation effect is not clearly observed. If the wave period is longer than 10.0 s, the passive heave compensator causes the increase of the heave motion of the manifold. This is because the shift of the resonance by the

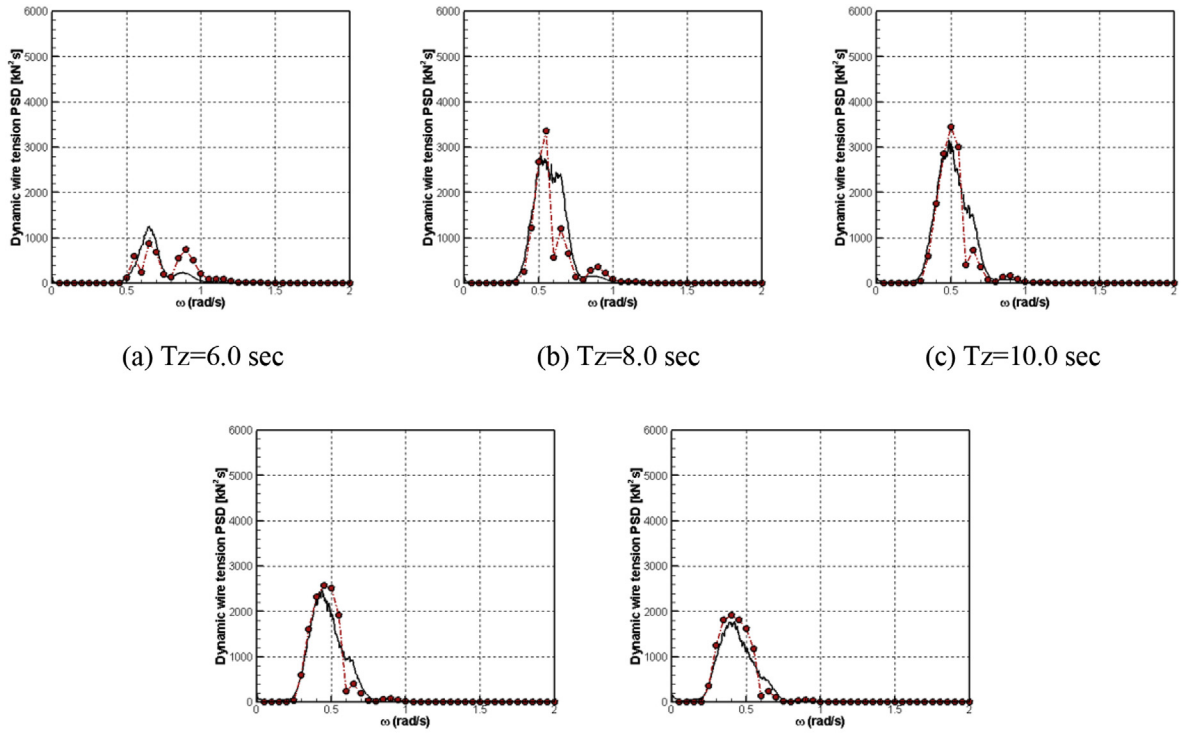

Fig. 26. Dynamic tension spectra of the hoisting wire in irregular waves.

Please cite this article in press as: Nam, B.W., et al., Experimental and numerical study on coupled motion responses of a floating crane vessel and a lifted subsea manifold in deep water, International Journal of Naval Architecture and Ocean Engineering (2017), http://dx.doi.org/10.1016/j.ijnaoe.2017.01.002

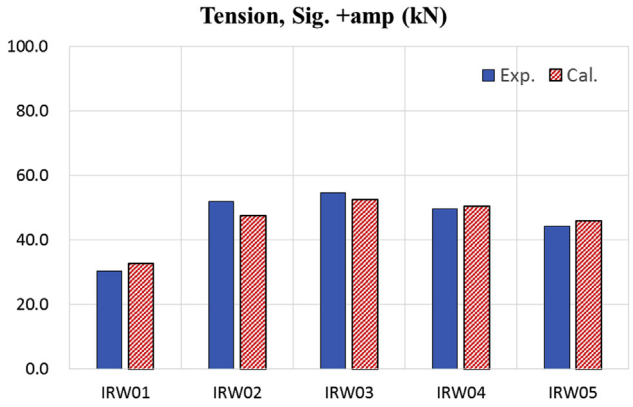

Fig. 27. Comparison of tension responses of the hoisting wire under the irregular wave conditions (water depth = −700 m).

usage of PHC results in high heave motion under the long wave period conditions. However, dynamic tension values is clearly reduced due to the usage of PHC. In particular, when the wave period is less than 10.0 s, the PHC reduces the dynamic tension of the hoisting wire by about 30–50%. The calculations results, shown in Fig. 31(b), also reveals the PHC effect on heave motion and tension responses. However, the tension reduction effect due to the PHC usage is relatively smaller rather than the experimental data. This is mainly attribute to the discrepancy of the tension responses in low-frequency range.

5. Conclusions

An experimental and numerical study was conducted for investigating deepwater crane installation operation of the

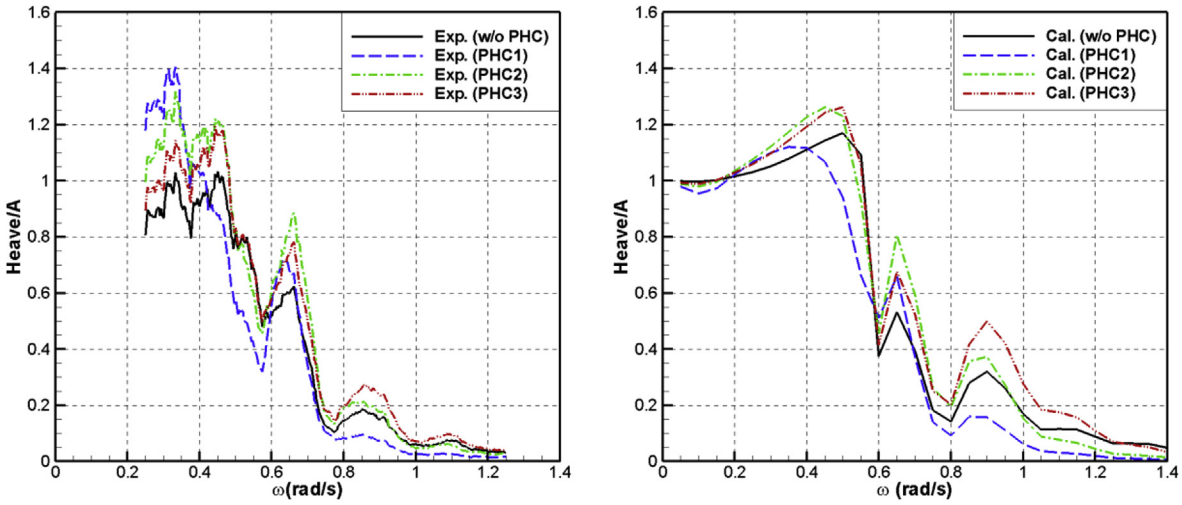

Fig. 28. Effect of the passive heave compensator on heave RAOs of the manifold.

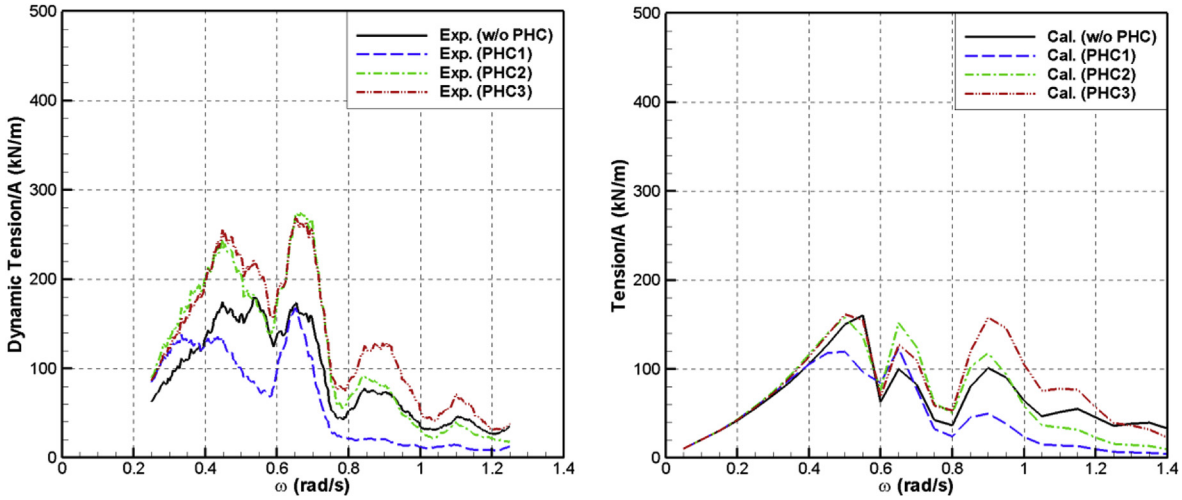

Fig. 29. Effect of the passive heave compensator on dynamic tension RAOs of the hoisting wire.

Please cite this article in press as: Nam, B.W., et al., Experimental and numerical study on coupled motion responses of a floating crane vessel and a lifted subsea manifold in deep water, International Journal of Naval Architecture and Ocean Engineering (2017), http://dx.doi.org/10.1016/j.ijnaoe.2017.01.002

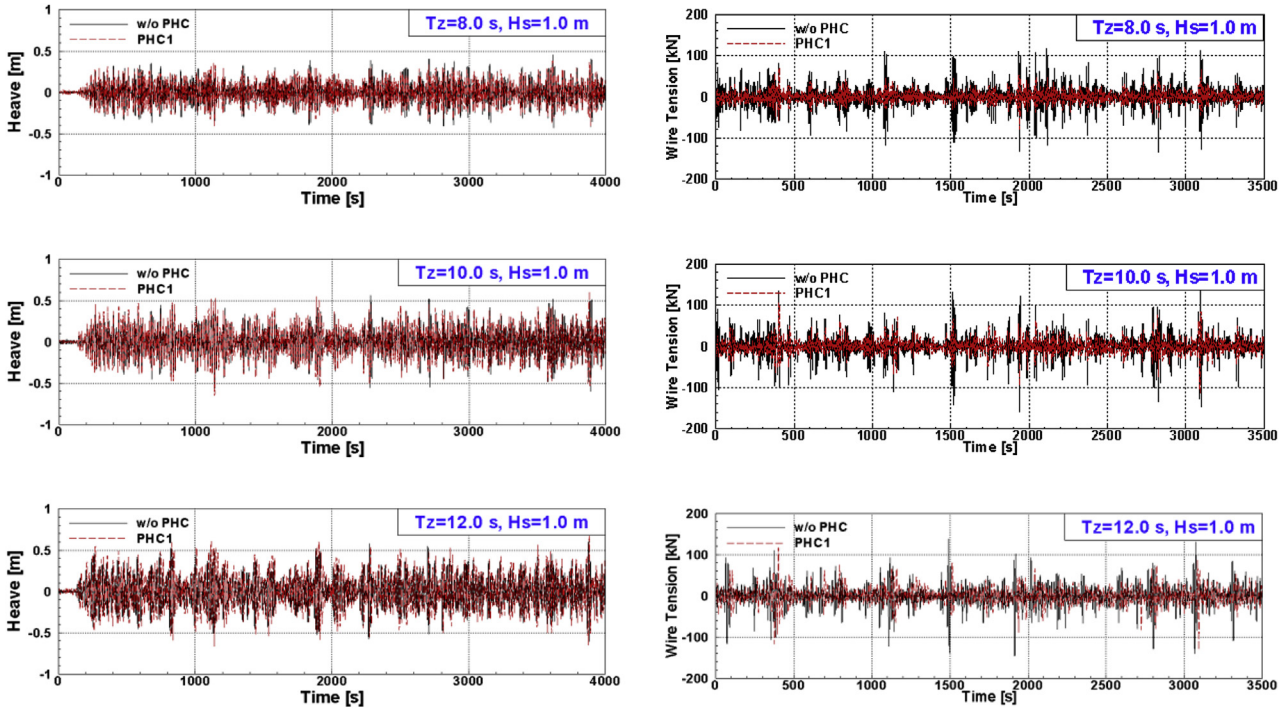

Fig. 30. Comparison of the manifold heaves and the wire tensions in irregular waves due to the passive heave compensator.

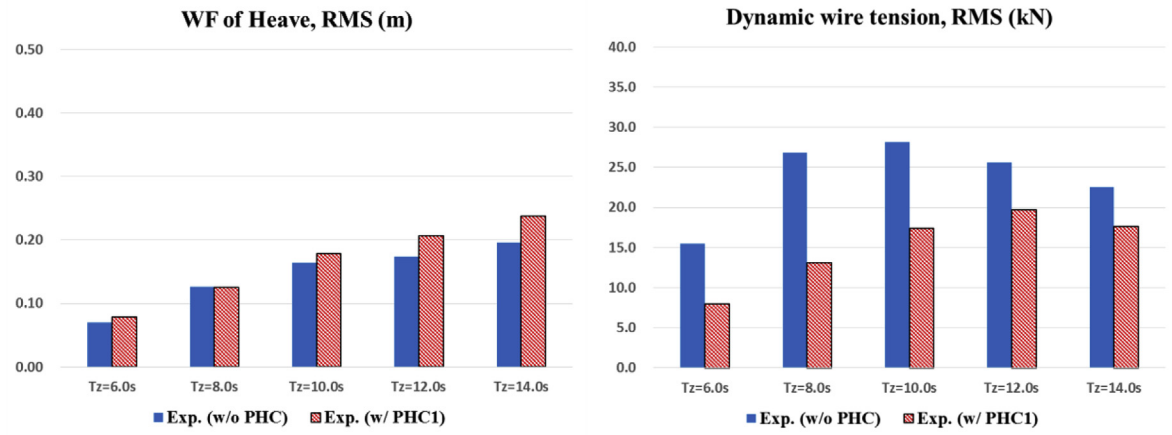

(a) Experiments

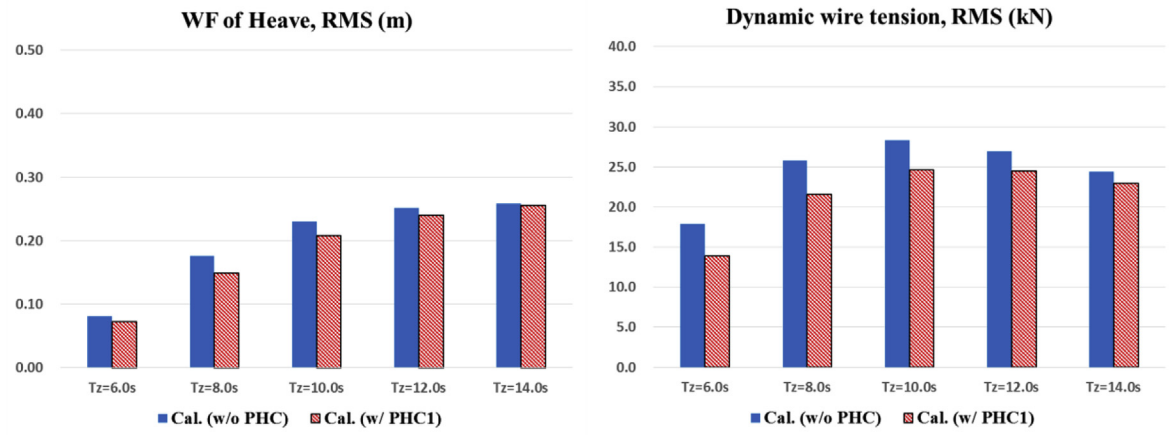

(b) Calculations

Fig. 31. Comparison of heave RMS of the manifold and dynamic tension RMS of the hoisting wire due to the passive heave compensator under five different irregular wave conditions.

Please cite this article in press as: Nam, B.W., et al., Experimental and numerical study on coupled motion responses of a floating crane vessel and a lifted subsea manifold in deep water, International Journal of Naval Architecture and Ocean Engineering (2017), http://dx.doi.org/10.1016/j.ijnaoe.2017.01.002

subsea equipment in waves. From a series of model tests and numerical calculations, the following conclusions are drawn.

- The crane vessel experience the significant roll motions even in the head waves because the interaction with the lifted object via the hoisting wire tension brings about the roll motions of the vessel. These roll motions are greatly affected by the weight of the lifted object.
- Heave motion of the lifted subsea manifold reveals three peak responses which is mainly caused by crane-tip motion and the vertical resonance of the hoisting system. The heave motion are strongly affected by the added-mass and hydrodynamic damping of the lifted object.
- The dynamic tension responses of the hoisting wire are greatly changed by the hydrodynamic coefficient of the lifted object. Maximum dynamic tension happens at the pitch and roll resonant conditions.
- The effect of passive heave compensator is clearly observed during deep-water lifting operations It is confirmed that the passive heave compensator shifts the resonant frequency of the hoisting system to the low frequency range. For short wave periods, the efficiency of the passive heave compensator is maximized in reducing dynamic tension of hoisting wire.
- The present calculation method in frequency domain shows fairly good agreement with the experimental data. Some discrepancies are found especially at high frequency ranges, where nonlinear damping characteristics is significant. In the future, nonlinear time-domain simulations with nonlinear drag model will be carried out to evaluate the nonlinear coupled dynamics between the crane vessel and the lifted object.

Acknowledgements

This research has been partly funded by a Grand-in-Aid for Strategy Technology Development Programs from the Korea Ministry of Trade, Industry & Energy (No. 10038598, "Development of deep water installation design and analysis technology" & No. 10042452, "Engineering Technology Development for the 3,000 m Deepwater Subsea Equipment and URF Installation to advance to Deepwater Offshore Plant Market").

References

Clauss, G.F., Vannahme, M., Ellermann, K., Kreuzer, E., 2000. Subharmonic oscillations of moore floating cranes. In: Proc Offshore Technology Conference, Houston, OTC-11953.

DNV, 2011. Modelling and Analysis of Marine Operation. DNV-RP-H103.

Fujarra, A.L.C., Tannuri, E.A., Masetti, I.Q., Igreja, H., 2008. Experimental and numerical evaluation of the installation of subsea equipments for risers support. In: Pro Int Conf on Offshore Mechanics and Arctic Eng, Honolulu, OMAE 2008–57472.

Galgoul, N.Z., Labanca, E.L., Claro, C.A., 2001. Experience gained during the istallation design of the poncador manifold in a 1860m water depth. In: Prc Int Conf on Offshore Mechanics and Arctic Eng, Rio de Janeiro, Brazil, OMAE 2001/OTF-1063.

Kimiaei, M., JiaJing, X., Yu, H., 2009. Comparing the results of a simplified numerical model with DNV guidelines for installation of subsea platforms. In: Prc Int Conf on Offshore Mechanics and Arctic Eng, Honolulu, OMAE 2009–79356.

Legras, J.L., Wang, J., 2011. Criteria for the operation of lowering a structure to the seabed based on the installation vessel motion. In: Proc Offshore Technology Conference, Houston, OTC-21250.

Nam, B.W., Hong, S.Y., Kim, Y.S., Kim, J.W., 2013. Effects of passive and active heave compensators on deepwater lifting operation. Int J Offshore Polar Eng 23 (1), 33–37.

Nam, B.W., Kim, N.W., Choi, Y.M., Hong, S.Y., Kim, J.W., 2015. An experimental study on deepwater crane installation of subsea equipment in waves. In: Proc of Int Offshore and Polar Eng Conf, Kona, Big Island, Hawaii, USA, pp. 1279–1283.

Park, Y.S., Kim, W.J., Nam, B.W., 2013. CFD simulation of hydrodynamic forces acting on subsea manifold templates at wave zone. In: Proc of Int Offshore and Polar Eng Conf, Anchorage, Alaska, USA, pp. 654–661.

Vries, J.P., Drunen, Dijk, R., Zoontjes, R., 2011. Offshore monitoring campaign on installation of suction piles in deep water fields. In: Proc Offshore Technology Conference, Houston, OTC-21291.

Wang, J., Hagen, R.K., Radan, E., Bullock, J., 2011. Technical challenges and success for rigid pipeline with PLET, jumper and flying leads installation in conger 9 field. In: Proc Offshore Technology Conference, Houston, OTC-21209.

Please cite this article in press as: Nam, B.W., et al., Experimental and numerical study on coupled motion responses of a floating crane vessel and a lifted subsea manifold in deep water, International Journal of Naval Architecture and Ocean Engineering (2017), http://dx.doi.org/10.1016/j.ijnaoe.2017.01.002